

The Josephson frequency of resonantly coupled atomic and molecular condensates

R A Duine and H T C Stoof

Institute for Theoretical Physics, University of Utrecht, Leuvenlaan 4,
3584 CE Utrecht, The Netherlands

E-mail: duine@phys.uu.nl and stoof@phys.uu.nl

New Journal of Physics **5** (2003) 69.1–69.11 (<http://www.njp.org/>)

Received 13 March 2003, in final form 9 May 2003

Published 13 June 2003

Abstract. Motivated by recent experiments (Claussen *et al* 2003 *Preprint* cond-mat/0302195) we investigate the magnetic-field dependence of the Josephson frequency of coherent atom–molecule oscillations near a Feshbach resonance. Far off resonance this frequency is determined by two-atom physics. However, the Josephson frequency is relatively large in this case and a description purely in terms of scattering lengths turns out to be inadequate. In particular, we have to include the effective range parameter of the interatomic interaction in our calculations. Close to resonance, the frequency deviates from the two-body results due to various many-body shifts. Considering also the many-body effects, we find perfect agreement with the experimental results over the entire range of magnetic field.

Contents

1	Introduction	2
2	Atom–molecule coherence	2
2.1	Microscopic theory	3
2.2	Ladder diagrams	3
3	Molecular binding energy	6
4	Josephson oscillations	7
5	Conclusions	10
	Acknowledgment	10
	References	10

1. Introduction

The collisional properties of ultracold alkali atoms are strongly affected by the presence of a bound state in a coupled closed channel when the energy of that bound state is close to the energy of the two colliding atoms. This situation is called a Feshbach resonance [1]–[3] and is currently of great experimental interest, because the energy difference between the two colliding atoms and the molecular bound state is magnetic-field dependent due to the different Zeeman shifts of the atoms in the open channel and the molecule. This leads to a high level of experimental control over the interatomic interactions [4].

The physics of a Feshbach resonance bears some similarity with an ordinary quantum mechanical two-level system, where one level represents the two atoms and the other level the molecular state. Inspired by this picture, Donley *et al* [5] have conducted a Ramsey-type experiment, by starting from an essentially pure atomic condensate and applying two short pulses in the magnetic field separated by a longer evolution time. As a function of the evolution time, oscillations in the number of remaining condensate atoms are observed. Sufficiently far from resonance the frequency corresponds to the molecular binding energy, in agreement with the fact that in that case the coupling may be neglected and the Josephson frequency of the oscillations between an atomic and a molecular Bose–Einstein condensate is equal to the energy difference between the two atoms and the molecule. More recent high-precision experiments by Claussen *et al* [6], over a larger range of magnetic fields, have shown that close to the resonance the frequency deviates from the two-body result as a result of many-body effects.

In order to be able to theoretically describe the magnetic-field dependence of the observed frequency of coherent atom–molecule oscillations over a large range of magnetic field, we have to incorporate into the many-body theory the relevant two-atom physics exactly, and, in particular therefore, the correct molecular binding energy. Far off resonance this binding energy is relatively large and it turns out to be necessary to include the energy dependence of the interactions and coupling constants in the theoretical description. In particular, the use of solely the scattering length is inadequate and we also need to include the effective range of the interatomic interaction potential. In addition, to describe the deviation from the two-body result close to resonance, the theory has to incorporate the correct mean-field interactions between condensate and noncondensate atoms that ultimately give rise to mean-field shifts of the molecule. Although a large number of important contributions have been made in formulating a theory for Feshbach-resonant interactions [7]–[13], it appears that none of the existing theories provides a quantitative agreement with the experimentally observed Josephson frequency over the full range of the magnetic field. It is the aim of this paper to put forward such a theory and thereby also improve upon our previous calculations which were restricted to the region close to resonance where many-body effects are observed [14].

To this end, the paper is organized as follows. In section 2 we first present the many-body theory that incorporates the molecular binding energy exactly. This theory includes the effective range of the interatomic interactions, which is determined from experiment in section 3 by calculating the molecular binding energy in vacuum. In section 4 we calculate the frequency of the coherent atom–molecule oscillations, i.e., the Josephson frequency that includes the many-body shifts of the two-body results. We end in section 5 with our conclusions.

2. Atom–molecule coherence

In this section we present the theory for the description of Feshbach-resonant interactions between atoms. The theory presented here improves upon our results presented in [13] by including the

energy dependence of the various coupling constants and, in particular therefore, the effective range of the atom–atom interactions.

2.1. Microscopic theory

Our starting point is the microscopic atom–molecule Hamiltonian for the description of a Feshbach resonance [13]. For a homogeneous system in a box of volume V this Hamiltonian reads

$$\hat{H} = \sum_{\mathbf{k}} \epsilon_{\mathbf{k}} \hat{a}_{\mathbf{k}}^{\dagger} \hat{a}_{\mathbf{k}} + \frac{1}{2V} \sum_{\mathbf{K}, \mathbf{k}, \mathbf{k}'} V(\mathbf{k} - \mathbf{k}') \hat{a}_{\mathbf{K}/2+\mathbf{k}}^{\dagger} \hat{a}_{\mathbf{K}/2-\mathbf{k}}^{\dagger} \hat{a}_{\mathbf{K}/2+\mathbf{k}'} \hat{a}_{\mathbf{K}/2-\mathbf{k}'} \\ + \sum_{\mathbf{k}} \left[\frac{\epsilon_{\mathbf{k}}}{2} + \delta_{\text{B}}(B) \right] \hat{b}_{\mathbf{k}}^{\dagger} \hat{b}_{\mathbf{k}} + \frac{1}{\sqrt{V}} \sum_{\mathbf{K}, \mathbf{k}} g_{\text{B}}(\mathbf{k}) [\hat{b}_{\mathbf{K}}^{\dagger} \hat{a}_{\mathbf{K}/2+\mathbf{k}} \hat{a}_{\mathbf{K}/2-\mathbf{k}} + \text{H.c.}]. \quad (1)$$

Here, the operator $\hat{a}_{\mathbf{k}}^{\dagger}$ creates an atom with momentum $\hbar \mathbf{k}$, and its Hermitian conjugate (H.c.) annihilates an atom with this momentum. The single-atom dispersion is given by $\epsilon_{\mathbf{k}} = \hbar^2 \mathbf{k}^2 / 2m$. The molecules are described by the operators $\hat{b}_{\mathbf{k}}^{\dagger}$ and $\hat{b}_{\mathbf{k}}$ and have a single-particle dispersion given by $\epsilon_{\mathbf{k}}/2 + \delta_{\text{B}}(B)$ since their mass is twice the atomic mass m . Here $\delta_{\text{B}}(B)$ is the detuning of the bare molecules, i.e., the energy difference between the bare molecules and the atoms, which depends on the magnetic field B due to the fact that the magnetic moment of the molecule is different from that of the atoms. The Fourier transform of the atom–atom interaction in the incoming channel is given by $V(\mathbf{k})$, and goes to zero as $\mathbf{k} \rightarrow \infty$ due to the nonzero range of the atomic interactions. The bare atom–molecule coupling is given by $g_{\text{B}}(\mathbf{k})$ and also goes to zero as $\mathbf{k} \rightarrow \infty$, due to the fact that the wavefunction of the bare molecule has a finite, nonzero extent. The atom–molecule interactions as well as the molecule–molecule interactions have been neglected, because we are interested in the Josephson oscillations of an almost pure atomic condensate.

In applying the above microscopic Hamiltonian to realistic atomic gases we have to use perturbation theory in the atom–atom interaction and the atom–molecule coupling. These quantities are large and we have to consider them to all orders. At the low densities of interest to us here, we need only to consider all ladder diagrams, since processes involving three and more bodies are negligible. This automatically builds into our theory the relevant two-atom physics, i.e., the scattering amplitude of the atoms and the binding energy of the molecule. Note that the fact that both the atom–molecule coupling and the atom–atom interaction decrease rapidly with increasing momenta ensures that no ultraviolet divergences are encountered when using perturbation theory for these quantities. In the next section we discuss the required perturbative expansion.

2.2. Ladder diagrams

First, we consider the atom–atom scattering amplitude. To lowest order in the interaction the amplitude of two atoms scattering from relative momentum $\hbar \mathbf{k}'$ to relative momentum $\hbar \mathbf{k}$ is simply equal to $V(\mathbf{k} - \mathbf{k}')$. However, since this interaction is strong we have to consider also the situation where the atoms collide twice, three times and so on. Diagrammatically, this leads to the Born series shown in figure 1(a), which is summed by introducing the many-body T -matrix (transition matrix) that obeys the Bethe–Salpeter equation

$$T^{\text{MB}}(\mathbf{k}, \mathbf{k}', \mathbf{K}, z) = V(\mathbf{k} - \mathbf{k}') + \frac{1}{V} \sum_{\mathbf{k}''} V(\mathbf{k} - \mathbf{k}'') \frac{[1 + N(\epsilon_{\mathbf{K}/2+\mathbf{k}''} - \mu) + N(\epsilon_{\mathbf{K}/2-\mathbf{k}''} - \mu)]}{z - \epsilon_{\mathbf{K}/2+\mathbf{k}''} - \epsilon_{\mathbf{K}/2-\mathbf{k}''}} \\ \times T^{\text{MB}}(\mathbf{k}'', \mathbf{k}', \mathbf{K}, z). \quad (2)$$

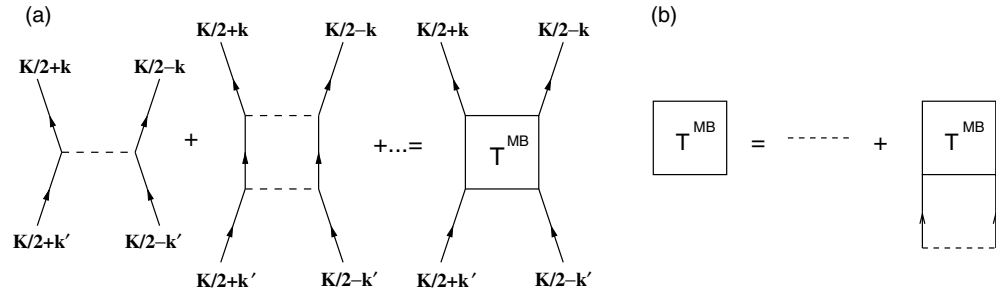


Figure 1. (a) The Born series for the scattering amplitude. (b) The diagrammatic representation of the many-body T -matrix. The solid lines correspond to single-atom propagators. The dashed lines correspond to the interatomic interaction $V(k)$.

Here we have used the Hartree–Fock approximation for the thermal atoms and, for the moment, neglected mean-field shifts. Furthermore, $N(x) = [e^{\beta x} - 1]^{-1}$ is the Bose distribution function of the atoms, μ their chemical potential and $\beta = 1/k_B T$ the inverse thermal energy. The total energy at which the scattering takes place is denoted by z . Due to the surrounding medium the scattering amplitude depends also on the centre-of-mass momentum \mathbf{K} of the colliding atoms. The diagrammatic representation of this equation is given in figure 1(b).

For temperatures not too close to the critical temperature we are allowed to neglect the many-body effects [15] and (2) reduces to the Lippmann–Schwinger equation for the two-body T -matrix. The effective scattering amplitude thus becomes $T^{2B}(\mathbf{k}, \mathbf{k}', z - \epsilon_K/2)$. For the small external momenta of interest to us here the momentum dependence of the two-body T -matrix may be neglected. Its energy dependence, however, cannot be neglected, since we are ultimately interested in calculating the molecular binding energy which is relatively large far off resonance. Including the energy dependence of the T -matrix [16], we thus conclude that the renormalization of the amplitude for two atoms scattering at the physically relevant energy $\hbar\omega^+ \equiv \hbar\omega + i0$ is given by

$$V(\mathbf{k} - \mathbf{k}') \rightarrow T^{2B}(\mathbf{0}, \mathbf{0}, \hbar\omega^+) = \frac{4\pi a_{bg} \hbar^2}{m} \left[\frac{1}{1 + i a_{bg} \sqrt{\frac{m\omega}{\hbar}} - \frac{a_{bg} r_{bg} m\omega}{2\hbar}} \right]. \quad (3)$$

Here a_{bg} denotes the s-wave scattering length of the potential $V(\mathbf{k})$, which, due to the fact that it describes the nonresonant part of the atomic interactions, is called the background scattering length. The parameter r_{bg} is, by definition, the effective range of this potential.

Next, we calculate the amplitude for two atoms with momenta $\hbar \mathbf{K}/2 + \hbar \mathbf{k}$ and $\hbar \mathbf{K}/2 - \hbar \mathbf{k}$ to form a molecule with energy z . To lowest order in the atomic interaction this amplitude is equal to $g_B(\mathbf{k})$. However, before forming a molecule, the two atoms may undergo multiple collisions and we again have to take into account the full Born series, diagrammatically given in figure 2(a), which is summed by again introducing the many-body T -matrix as shown in figure 2(b). This leads to the equation

$$g^{MB}(\mathbf{k}, \mathbf{K}, z) = g_B(\mathbf{k}) + \frac{1}{V} \sum_{\mathbf{k}'} T^{MB}(\mathbf{k}, \mathbf{k}', \mathbf{K}, z) \times \frac{[1 + N(\epsilon_{K/2+k'} - \mu) + N(\epsilon_{K/2-k'} - \mu)]}{z - \epsilon_{K/2+k'} - \epsilon_{K/2-k'}} g_B(\mathbf{k}'). \quad (4)$$

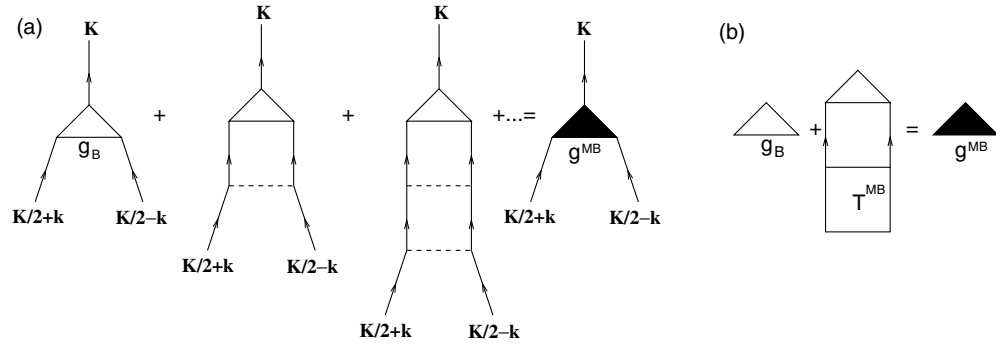


Figure 2. Diagrammatic calculation of the amplitude of two atoms to form a molecule. The open and filled triangles represent the bare and many-body constants of coupling between the atoms and the molecule, respectively.

Neglecting many-body effects, the amplitude becomes $g^{2B}(\mathbf{k}, z - \epsilon_K/2)$ with

$$g^{2B}(\mathbf{k}, z) = g_B(\mathbf{k}) + \frac{1}{V} \sum_{\mathbf{k}'} T^{2B}(\mathbf{k}, \mathbf{k}', z) \frac{1}{z - 2\epsilon_{\mathbf{k}'}} g_B(\mathbf{k}'). \quad (5)$$

From the above equation we infer that the energy dependence of the amplitude is the same as that of the two-body T -matrix. This result is easily understood by noting that for a contact potential $V(\mathbf{k}) = V_0$ and we simply have that $g^{2B} = g_B T^{2B}/V_0$. Hence we have for the renormalization of the amplitude for forming a molecule with energy $\hbar\omega$ the expression

$$g_B \rightarrow g^{2B}(\mathbf{0}, \hbar\omega^+) = g \left[\frac{1}{1 + i a_{bg} \sqrt{\frac{m\omega}{\hbar}} - \frac{a_{bg} r_{bg} m\omega}{2\hbar}} \right], \quad (6)$$

where g is the atom–molecule coupling constant at zero energy.

Finally, we have to take into account the fact that the coupling between the atoms and the molecule gives the molecule a finite lifetime and leads to a change in the bound-state energy of the molecule. Physically, this is described by the self-energy of the molecules which, within our approximations, is equal to $\hbar \Sigma_m^{2B}(z - \epsilon_K/2)$ with

$$\hbar \Sigma_m^{2B}(z) = 2 \int \frac{d\mathbf{k}}{(2\pi)^3} |g^{2B}(\mathbf{0}, 2\epsilon_{\mathbf{k}})|^2 \frac{1}{z - 2\epsilon_{\mathbf{k}}}. \quad (7)$$

This expression is most easily understood by considering the fact that evaluated at positive energy $\hbar\omega^+$ and using $\text{Im}[1/(\omega^\pm - \omega')] = \mp\pi\delta(\omega - \omega')$, it immediately leads to the correct Fermi golden rule for the decay rate of the molecule. Using the result for the amplitude in equation (6) the retarded self-energy $\hbar \Sigma_m^{(+)}(\hbar\omega)$, i.e., the self-energy evaluated at energy $\hbar\omega^+$, becomes

$$\hbar \Sigma_m^{(+)}(\hbar\omega) = - \frac{g^2 m}{2\pi \hbar^2 \sqrt{1 - 2 \frac{r_{bg}}{a_{bg}}}} \left[\frac{i \sqrt{(1 - 2 \frac{r_{bg}}{a_{bg}}) \frac{m\omega}{\hbar}} - \frac{r_{bg} m\omega}{2\hbar}}{1 + i a_{bg} \sqrt{(1 - 2 \frac{r_{bg}}{a_{bg}}) \frac{m\omega}{\hbar}} - \frac{r_{bg} a_{bg} m\omega}{2\hbar}} \right], \quad (8)$$

where we have for simplicity assumed that the background scattering length is negative, which is the case for the applications of interest here. We have also subtracted the $z = 0$ part in the integral in equation (7) since this shift renormalizes the bare detuning according to $\delta_B(B) \rightarrow \delta(B)$. Note that the square-root behaviour of $\hbar \Sigma_m^{(+)}(\hbar\omega)$ at small energies is in agreement with the expected Wigner-threshold law for the molecule decaying into the two-atom continuum.

At this point we make the connection with experimentally known parameters. The resonance is characterized experimentally by a width ΔB and a position B_0 . More precisely, the s-wave scattering length of the atoms as a function of magnetic field is given by

$$a(B) = a_{\text{bg}} \left(1 - \frac{\Delta B}{B - B_0} \right). \quad (9)$$

Therefore, in order to reproduce the experimentally observed width of the resonance we have that $g = \hbar \sqrt{2\pi a_{\text{bg}} \Delta B \Delta \mu / m}$, since an elimination of the molecular field shows that $a_{\text{bg}} \Delta B = mg^2 / (2\pi \hbar^2 \Delta \mu)$. We have made use of the fact that the detuning is given by $\delta(B) = \Delta \mu (B - B_0)$ where $\Delta \mu$ is the difference in magnetic moment between two atoms and a bare molecule.

In this paper we focus on the experiments by Claussen *et al* [6]. In these experiments the Feshbach resonance at $B_0 = 155.041(18)$ G in the $|f = 2; m_f = -2\rangle$ state of ^{85}Rb is used. The width of the resonance is equal to $\Delta = 10.71(2)$ G and the background scattering length is $a_{\text{bg}} = -443 a_0$ with a_0 the Bohr radius. The difference in magnetic moment between two atoms and the bare molecule is equal to $\Delta \mu = -2.23 \mu_B$ with μ_B the Bohr magneton [10]. In the next section we also determine the effective range of the atom–atom interactions by calculating the binding energy of the molecule and comparing the result with experiment.

3. Molecular binding energy

The molecular bound-state energy is determined by solving for $\hbar\omega$ in the equation

$$\hbar\omega = \delta(B) + \hbar \Sigma_m^{(+)}(\hbar\omega). \quad (10)$$

For positive detuning this leads to an imaginary bound-state energy, in agreement with the fact that the molecule decays when its energy is above the threshold of the two-atom continuum. For negative detuning there is a bound state with energy $\epsilon_m(B)$. Close to resonance we are allowed to neglect the contribution from the effective range to the self-energy in equation (8) and we solve (10) analytically to find

$$\epsilon_m(B) \simeq -\frac{\hbar^2}{m[a(B)]^2}. \quad (11)$$

This is indeed the correct result for the molecular bound-state energy close to resonance [10].

Far off resonance, we are no longer allowed to neglect the effective range of the interatomic interaction. Because of this, the equation for the bound-state energy cannot be solved analytically any longer, but is nevertheless easily solved numerically. In order to determine the effective range we compare the result with the experimental results of Claussen *et al* [6]. In these experiments the Josephson oscillation frequency for coherent atom–molecule oscillations is determined as a function of the magnetic field. Far off resonance this frequency is essentially equal to the molecular binding energy and therefore independent of the condensate density. By comparing our results with the experimental data far off resonance, we determine the effective range uniquely. In figure 3 we show the binding energy as a function of the magnetic field. The solid curve is the result of a calculation with $r_{\text{bg}} = 185 a_0$. The dashed curve shows the result for zero effective range and the dotted curve shows the magnetic-field dependence given in (11). The experimental points, taken from [6], are also shown. It should be noted that the error bars on the experimental data are roughly indicated by the size of the points. Clearly, the result

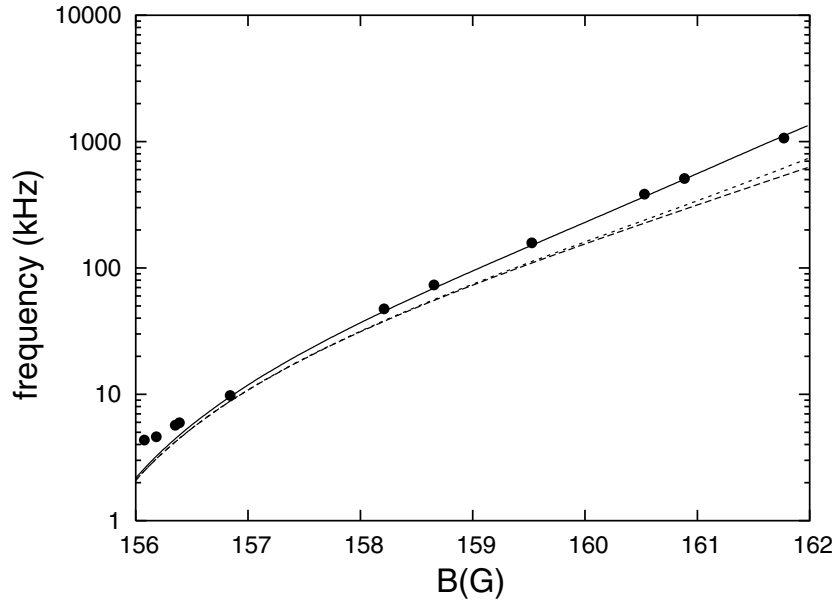


Figure 3. The molecular binding energy in vacuum. The solid curve shows the result of a calculation with $r_{bg} = 185 a_0$; the dashed curve shows the result for $r_{bg} = 0$. The dotted curve shows $|\epsilon(B)| = \hbar^2 / m a^2$. The experimental points are taken from [6].

with zero effective range as well as the expression given in equation (11) deviate significantly from the experimental data for magnetic fields larger than 158 G. Interestingly, the result for zero effective range deviates more from the experimental result than the expression given by equation (11). The curve obtained with an effective range of $r_{bg} = 185 a_0$ agrees very well with the experimental data in the regime where $B > 157$ G and hence we use this value for the effective range of the interatomic interaction from now on. As expected, close to the resonance, the results of the three calculations become identical because the energy dependence of the effective interactions becomes less important in this regime. Note, however, that all three results deviate from the experimental points for magnetic fields smaller than 157 G. This deviation is explained by considering many-body effects which are the topic of the next section.

4. Josephson oscillations

To determine the Josephson frequency of coherent oscillations between the atomic and the molecular condensate we calculate the excitation spectrum of the system by means of linear response theory. Therefore, we write for the atomic and molecular Heisenberg creation operators

$$\begin{aligned}\hat{a}_k(t) &= [\sqrt{N_a} + u_k e^{-i\omega t} \hat{\alpha}_k - v_{-k} e^{+i\omega t} \hat{\alpha}_k^\dagger] e^{-i\mu t/\hbar}, \quad \text{and} \\ \hat{b}_k(t) &= [\sqrt{N_m} + u'_k e^{-i\omega t} \hat{\beta}_k - v'_{-k} e^{+i\omega t} \hat{\beta}_k^\dagger] e^{-i2\mu t/\hbar},\end{aligned}\tag{12}$$

respectively. The operators $\hat{\alpha}_k$ and $\hat{\beta}_k$ describe a Bogoliubov quasi-atom and quasi-molecule, respectively, and in linear response theory we keep terms up to quadratic order in these operators. The number of particles in the atomic and molecular condensate is in equilibrium equal to N_a and N_m , respectively. In the presence of an atomic condensate it is crucial to take into account

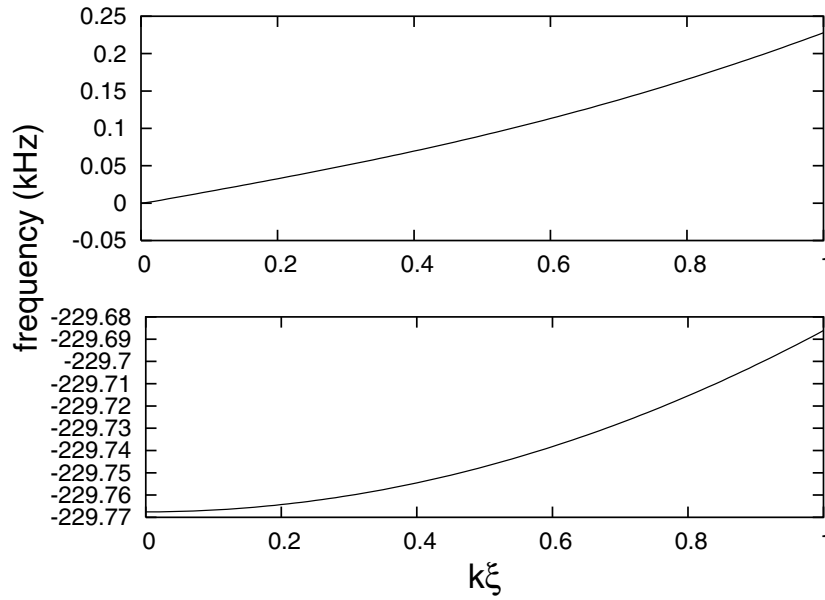


Figure 4. The dispersion relation of the collective modes of an atom–molecule system for a condensate density of $n_a = 2 \times 10^{12} \text{ cm}^{-3}$ at a magnetic field of $B = 160 \text{ G}$. The upper branch corresponds to the gapless dispersion for phonons. The lower branch corresponds to coherent atom–molecule oscillations. The momentum is indicated in units of the inverse coherence length $\xi^{-1} = \sqrt{16\pi an_a}$.

its mean-field effects on the thermal atoms. This mean-field energy is, in the Hartree–Fock approximation, given by

$$\hbar \Sigma^{\text{HF}} = 2n_a \left(T^{2\text{B}}(\mathbf{0}, \mathbf{0}, \mu - \hbar \Sigma^{\text{HF}}) + \frac{2|g^{2\text{B}}(\mathbf{0}, \mathbf{0}, \mu - \hbar \Sigma^{\text{HF}})|^2}{\hbar \Sigma^{\text{HF}} + \mu - \delta(B) - \hbar \Sigma_{\text{m}}^{(+)}(\mu - \hbar \Sigma^{\text{HF}})} \right), \quad (13)$$

and reduces to the usual expression $8\pi a(B)\hbar^2 n_a/m$ far off resonance. Here, $n_a \equiv N_a/V$ denotes the density of the atomic Bose–Einstein condensate.

To find the excitation spectrum, we have to diagonalize the Hamiltonian in terms of the Bogoliubov quasi-particle operators. This requires the diagonalization of a 4×4 matrix equation for the coherence factors u_k , v_k , u'_k and v'_k . However, the coherence factors for the molecular operators are straightforwardly eliminated. This yields the 2×2 eigenvalue problem given by

$$\begin{aligned} [T_{\text{eff}}^{2\text{B}}(2\mu)n_a]^* u_k + [\epsilon_k - \mu + 2T_{\text{eff}}^{2\text{B}}(2\mu - \hbar\omega - \epsilon_k/2)n_a]^* v_k &= -\hbar\omega v_k, \\ [\epsilon_k - \mu + 2T_{\text{eff}}^{2\text{B}}(2\mu + \hbar\omega - \epsilon_k/2)n_a] u_k + T_{\text{eff}}^{2\text{B}}(2\mu)n_a v_k &= \hbar\omega u_k, \end{aligned} \quad (14)$$

where the effective atom–atom interaction is given by

$$T_{\text{eff}}^{2\text{B}}(\hbar\omega) = T^{2\text{B}}(\mathbf{0}, \mathbf{0}, \hbar\omega^+ - 2\hbar \Sigma^{\text{HF}}) + \frac{2|g^{2\text{B}}(\mathbf{0}, \mathbf{0}, \hbar\omega^+ - 2\hbar \Sigma^{\text{HF}})|^2}{\hbar\omega^+ - \delta(B) - \hbar \Sigma_{\text{m}}^{(+)}(\hbar\omega - 2\hbar \Sigma^{\text{HF}})}. \quad (15)$$

The chemical potential is determined by the time-independent Gross–Pitaevskii equation, which, for energy-dependent interactions, reads

$$\mu = T_{\text{eff}}^{2\text{B}}(2\mu)n_a. \quad (16)$$

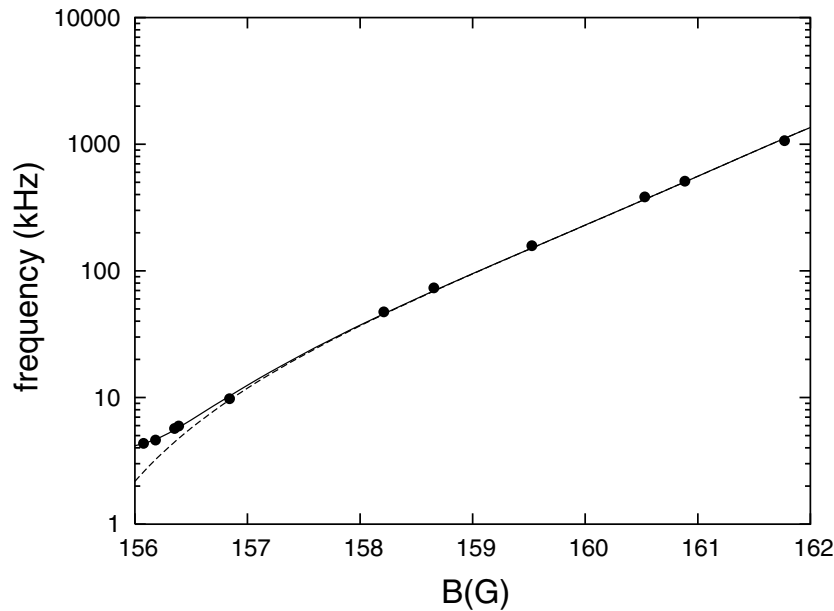


Figure 5. The Josephson frequency of coherent atom–molecule oscillations for an atomic condensate density of $n_a = 2 \times 10^{12} \text{ cm}^{-3}$. The solid curve shows the result of the calculation of the Josephson frequency. The dashed curve shows the molecular binding energy in vacuum. The experimental points are taken from [6].

Note that this last equation and equation (13) uniquely determine the chemical potential and the Hartree–Fock mean-field energy for a given atomic condensate density. Also note that it is crucial to include the Hartree–Fock mean-field shift to have equilibrium solutions. The number of molecules in the molecular condensate can be calculated from the number of condensate atoms, but is eliminated here to get the effective atom–atom interaction [14]. We find, depending on how close we are to resonance, that the equilibrium density of condensed bare molecules is at least three orders of magnitude smaller than the atomic condensate density. This justifies our neglect of the atom–molecule and molecule–molecule interactions since these give rise to mean-field effects that are at least three orders of magnitude smaller than the mean-field effects due to the atom–atom interaction that we have taken into account.

The dispersion relation of the collective excitations is found by solving the eigenvalue problem in equation (14) numerically. This yields two branches: one gapless branch corresponding to the phonon modes and a gapped branch corresponding to the atom–molecule oscillations. Physically, the difference between the two branches is understood by realizing that for the phonon modes the phases of the atomic and the molecular condensate are locked to each other and oscillate in phase. Since the Hamiltonian is invariant under transformations $\hat{a} \rightarrow \hat{a}e^{i\theta}$ and $\hat{b} \rightarrow \hat{b}e^{2i\theta}$ we conclude that the phonons are indeed gapless and, in fact, correspond to the Goldstone mode associated with the breaking of the $U(1)$ symmetry by the condensates. For the coherent atom–molecule oscillations the phases of the atomic and molecular condensate oscillate out of phase and hence the associated dispersion is gapped. Figure 4 shows the two branches of the dispersion for a condensate density of $n_a = 2 \times 10^{12} \text{ cm}^{-3}$ at a magnetic field of $B = 160 \text{ G}$.

The zero-momentum part of the gapped branch corresponds to the Josephson frequency of the coherent oscillations between the atomic and the molecular condensate, as observed by

Claussen *et al* [6]. In figure 5 the dotted curve shows the result of the calculation of this frequency for a condensate density of $n_a = 2 \times 10^{12} \text{ cm}^{-3}$. This density corresponds to the effective homogeneous density that we have to take in order to compare to the experimental results found by Claussen *et al* [6], which are performed in an inhomogeneous magnetic trap. Roughly speaking, this comes about because in the comparison of our homogeneous calculation with the inhomogeneous situation the effective Josephson coupling, which mostly determines the deviations from the two-body result, is reduced by an overlap integral of the atomic and molecular wavefunctions. This reduction factor multiplied by the experimental central density determines the effective homogeneous density [14]. Clearly, our result shows perfect agreement with the experimental data points over the entire experimentally investigated range of the magnetic field. The dashed curve in figure 5 corresponds to the molecular binding energy in vacuum, also shown in figure 3. As expected, the Josephson frequency becomes equal to the binding energy far off resonance.

5. Conclusions

We have improved upon our previous work [13, 14] in calculating the Josephson frequency of coherent atom–molecule oscillations. In doing so, we had to include the energy dependence of the interactions and, in particular, the effective range of the interatomic interactions. We have found excellent agreement with the available experimental results. We have not attempted to calculate the Josephson frequency with other existing theories, which all use the Hartree–Fock–Bogoliubov approximation [10]–[12]. However, this approximation does not contain the Hartree–Fock self-energy of the noncondensed atoms, which is crucial in our calculations.

In future work we intend to study the density and magnetic-field dependence of the Josephson frequency in more detail. Moreover, we also intend to perform calculations that go beyond the linear response theory presented here. In particular, we expect the frequency to remain the same but also to find damping of the Josephson oscillations due to the fact that, in a nonequilibrium situation with time-dependent detuning, a fraction of the molecules can rogue-dissociate into noncondensed atom pairs [11]. This process is described by the imaginary part of the molecular self-energy.

Acknowledgment

It is a pleasure to thank Neil Claussen for providing us with the experimental data obtained by the group of Carl Wieman.

References

- [1] Feshbach H 1962 *Ann. Phys., NY* **19** 287
- [2] Stwalley W C 1976 *Phys. Rev. Lett.* **37** 1628
- [3] Tiesinga E, Verhaar B J and Stoof H T C 1993 *Phys. Rev. A* **47** 4114
- [4] Inouye S, Andrews M R, Stenger J, Miesner H J, Stamper-Kurn D M and Ketterle W 1998 *Nature* **392** 151
- [5] Donley E A, Claussen N R, Thompson S T and Wieman C E 2002 *Nature* **417** 529
- [6] Claussen N R, Kokkelmans S J J M F, Thompson S T, Donley E A and Wieman C E 2003 *Preprint cond-mat/0302195*
- [7] Drummond P D, Kheruntsyan K V and He H 1998 *Phys. Rev. Lett.* **81** 3055
Kheruntsyan K V and Drummond P D 1998 *Phys. Rev. A* **58** R2676

- [8] Timmermans E, Tommasini P, Côté R, Hussein M and Kerman A 1999 *Phys. Rev. Lett.* **83** 2691
- [9] Holland M, Park J and Walser R 2001 *Phys. Rev. Lett.* **86** 1915
- [10] Kokkelmans S J J M F and Holland M 2002 *Phys. Rev. Lett.* **89** 180401
- [11] Mackie M, Suominen K A and Javanainen J 2002 *Phys. Rev. Lett.* **89** 180403
- [12] Köhler T, Gasenzer T and Burnett K 2002 *Phys. Rev. A* **67** 013601
- [13] Duine R A and Stoof H T C 2003 *J. Opt. B: Quantum Semiclass. Opt.* **5** S212
- [14] Duine R A and Stoof H T C 2003 *Preprint* cond-mat/0302304
- [15] Stoof H T C, Bijlsma M and Houbiers M 1996 *J. Res. Natl Inst. Stand. Technol.* **101** 443
- [16] See, for instance, Stoof H T C, de Goey L P H, Rovers W M H M, Kop Jansen P S M and Verhaar B J 1988 *Phys. Rev. A* **38** 1248